the quantum yield for this step is very high as compared with that of the first step (2).

The absorption peak of **1r** at ca. 356 nm and that of **2** at ca. 300 nm are due to the charge transfer from the bridging peroxide to cobalt(III).[23] Such a charge-transfer excited state should be involved in the photodeoxygenation. The d-d excited state does not seem to lead to deoxygenation.

The quantum yield of **1r** on irradiation at 356 nm is relatively low as compared with those reported for the redox decomposition of some mononuclear cobalt(III) complexes upon irradiation of the ligand-to-metal charge-transfer band.[24] It is 1 or 2 orders of magnitude lower than those for the decomposition of (μ-superoxo)dicobalt(III) complexes.[5,7]

Despite the low quantum yield, the photoinduced deoxygenation is interesting, since it indicates the photocontrolled reversible oxygen uptake. The reversibility is unfortunately not maintained in the present systems due to the slow irreversible photodecomposition of the binuclear species to mononuclear cobalt(III) complexes.

2. Irreversible Decomposition of 1r to Mononuclear Cobalt(III) Complexes. **1r** undergoes irreversible decomposition both thermally and photochemically, the thermal reaction being much slower and observed appreciably only at >50 °C. The mechanism of the thermal reaction is discussed first, since some relevant studies[11,25,26] permit more detailed discussion.

(a) The Thermal Reaction. A mononuclear (hydroperoxo)cobalt(III) complex was confirmed as an intermediate of the decomposition of $[(CN)_5Co^{III}(\mu\text{-}O_2^{2-})Co^{III}(CN)_5]^{6-}$ in neutral solution[25] and of $[(NO_2)(en)_2Co^{III}(\mu\text{-}O_2^{2-})Co^{III}(en)_2(NO_2)]^{2+}$ in acid solution.[26] Thus reaction 4[27] is likely to be the initial step of the decomposition of **1r**.

$$[(en)_2Co^{III}(\mu\text{-}OH,O_2^{2-})Co^{III}(en)_2]^{3+} \rightarrow [Co^{III}(en)_2(H_2O)_2]^{3+} + [Co^{III}(en)_2(O_2H)(H_2O)]^{2+} \quad (4)$$

In the absence of other ingredients, initially produced $[Co^{III}(en)_2(O_2H)(H_2O)]^{2+}$ would slowly react with coordinated ligand or ion-exchange resin during product analysis to give "orange species". Free ethylenediamine added to the solution of **1r** would be oxidized by $[Co^{III}(en)_2(O_2H)(H_2O)]^{2+}$. The decrease in decomposition rate in the presence of free ethylenediamine is not clearly accounted for.[28]

In the presence of both free ethylenediamine and Co^{II} ions, reaction 5[27] would take place.

$$[Co^{III}(en)_2(O_2H)(H_2O)]^{2+} + 2[Co^{II}(en)_n(H_2O)_{6-2n}]^{2+} \rightarrow [Co^{III}(en)_2(H_2O)_2]^{3+} + 2[Co^{III}(en)_n(H_2O)_{6-2n}]^{3+} \quad (5)$$

n = 2 or 3

(b) The Photochemical Decomposition. The reaction products contain various unidentified species. The reaction may be initiated by homolytic cleavage of the Co^{III}-(O_2Co^{III}) bond as is the thermal reaction. The reactive intermediate, Co^{III}-O_2^{2-}(H), would undergo further complicated reactions. It is also plausible that the photodecomposition may be initiated by the reaction of **1** with Co^{II} species, which is produced by the initial photoequilibration. Addition of free ethylenediamine considerably decreases the amount of Co^{II} species by shifting the equilibrium to the dimer side, and it would retard the photodecomposition.[28]

Finally, it should be pointed out that previous studies on (μ-peroxo)dicobalt(III) complexes with amines might have been affected by possible photochemical reactions and might require reexamination.

Acknowledgment. This work was supported by a Grant-in-Aid for Scientific Research (No. 58430010) to K.S. from the Ministry of Education, Science and Culture of Japan. The authors are indebted to Professors M. Ito and N. Mikami of this department of the use of an argon ion laser (Molectron 52B).

(23) Lever, A. B. P.; Gray, H. B. *Acc. Chem. Res.* **1978**, *11*, 348-355.
(24) Endicott, J. F. In "Concepts of Inorganic Photochemistry"; Adamson, A. W., Fleischauer, P. D., Eds.; Wiley: New York, 1975; pp 130-131.
(25) Bayston, J. H.; Looney, F. E.; Winifield, M. E. *Aust. J. Chem.* **1963**, *16*, 557-564.
(26) Shibahara, T.; Kuroya, H.; Mori, M. *Bull. Chem. Soc. Jpn.* **1980**, *53*, 2834-2838.
(27) The products of reactions 4 and 5 should be in equilibrium with their conjugate bases, hydroxo complexes, depending on the pH of the solution.
(28) One possible explanation for the effect of free ethylenediamine on the rate of decomposition is that the free ligand would replace the hydroxo bridge to give the μ-ethylenediamine complex, $[(en)_2Co^{III}(\mu\text{-}O_2^{2-},en)Co^{III}(en)_2]^{4+}$, which has been claimed to exist (Crawford, M.; Bedell, S. A.; Patel, R. I.; Young, L. W.; Nakon, R. *Inorg. Chem.* **1979**, *18*, 2075-2079). The observed slow decomposition rate would be understood if the μ-ethylenediamine complex were more stable toward a decomposition similar to reaction 4. Also the production of $[Co^{III}(en)_3]^{3+}$ is expected from the decomposition of the μ-en complex. The failure to observe any photodecomposition of **1r** in the presence of free ethylenediamine would be explained if the postulated μ-en complex were photostable. We are not fully convinced, however, of the existence of the μ-en complex under our experimental conditions. No appreciable change in the absorption spectrum of **1r** was observed on addition of free ethylenediamine, and no CD spectrum appeared on addition of (*R*)-propylenediamine in the dark (the μ-*R*-pn complex, if formed, would show some CD spectrum).

Contribution from the Department of Chemistry, Cornell University, Ithaca, New York 14853

Hypervalent Tellurium in One-Dimensional Extended Structures Containing Te_5^{n-} Units

JOEL BERNSTEIN† and ROALD HOFFMANN*

Received October 1, 1984

The electronic structure of three one-dimensional chains containing square-planar Te_5^{n-} units is presented, with employment of both molecular and band calculations. Two chains containing only Te_5^{2-} in different conformations and one in which they are modulated by Sn are treated. The Rb_2Te_5 or Cs_2Te_5 and K_2SnTe_5 structures are thus modeled. A three-center, four-electron model can be used to understand the elongation of the Te-Te bands within the Te_5 unit, whose inherent instability is overcome by the formation of the chains. It is suggested how oxidation of the chain, for instance, by suitable choice of synthetic conditions, would alter the geometric physical properties of these polymers.

The recent literature contains a number of examples of a square-planar tellurium structural unit which may formally be defined as Te_5^{n-} (**1**). In some cases such as Rb_2Te_5[1] and Cs_2Te_5[2] the stoichiometry clearly defines the charge on the unit as 2-. In these instances the unit is the basic building block of a one-di-

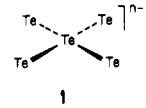

1

† Permanent address: Department of Chemistry, Ben-Gurion University of the Negev, Beer Sheva, Israel.

0020-1669/85/1324-4100$01.50/0

mensional anionic chain. In Cs_2Te_5 the Te_5^{n-} units are screw axis related (**2**) while in Rb_2Te_5 the Te_5^{n-} units are related by translation (**3**).

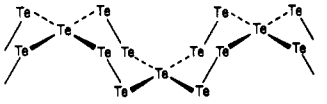

2

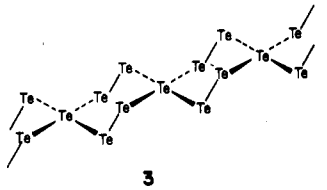

3

For most of the other cases in which the Te_5^{n-} unit appears, the attribution of a particular charge to the unit is more ambiguous. For instance, on K_2SnTe_5,[3] the unit again appears embedded in a one-dimensional chain (**4**) but the Te_5^{n-} units alternate

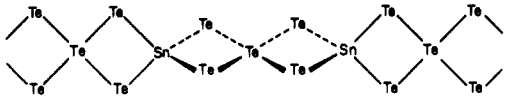

4

with tetrahedral Sn in making up the chain. Formally, at least, the square-planar units could still be considered Te_5^{2-} if the tin is Sn(0), but the Te–Sn bond length of 2.74 Å is almost identical with the sum of the tetrahedral covalent radii (2.72 Å) given by Pauling.[4] This suggests a formal oxidation state of 4+ for the Sn and a net charge of 6– on the Te_5^{n-} unit.

A similar ambiguity arises in the case of Ga_2Te_5,[5] although this is no longer a linear-chain structure but a three-dimensional one, as depicted in **5** in a view down the *c* axis of the tetragonal cell.

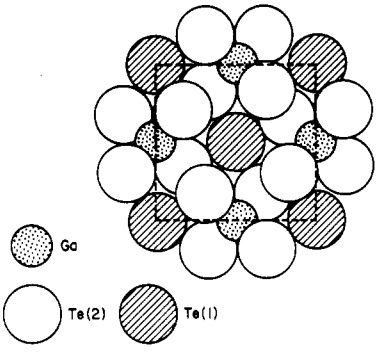

5

The Te_5 units are clearly present, with Te(1) as the central atom and four Te(2) atoms in the square-planar arrangement. The gallium is tetrahedrally surrounded by four Te(2) atoms. A choice of the "normal" valence state of Ga(III) leads to a formal charge of 6– on Te_5^{n-} while a choice of 2– for the charge on Te_5^{n-} would lead to an assignment of the only rarely encountered Ga(I).[6]

The structure of $AgTe_3$[7] (**6**) may also be visualized as being built up from Te_5^{n-} units (one such unit has been darkened) to

Table I. Geometric Features of the Te_5^{n-} Unit

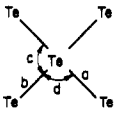

	a, Å	*b*, Å	*c*, deg	*d*, deg
Cs_2Te_5	3.046 (1)	...	90.5	89.5
Rb_2Te_5	3.039 (1)	...	92.0	88.0
K_2SnTe_5	3.015 (5)	3.052 (5)	95.0	88.2, 88.8
Ga_2Te_5	3.027 (2)	...	90.0	...
$AgTe_3$	3.052 (5)	...	89.8	89.8, 90.5
$NdTe_3$	3.076 (10)	...	90	
Re_2Te_5	2.983 (3)	3.022 (3)	91.2	88.8

give a rhombohedral structure, which is derived from the simple cubic α-polonium structure by a small perturbation.

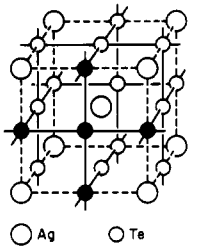

6

The structures of $NdTe_2$[8] and $NdTe_3$[9] also contain identifiable units of Te_5^{n-} where assignment of a formal charge is virtually ruled out by the complexity of the structures. Part of the $NdTe_3$ structure is shown in **7**.

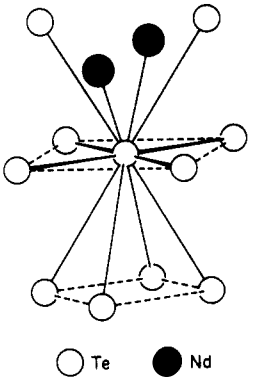

7

Finally, the fascinating structure of Re_2Te_5 has been reported by Klaiber, Petter, and Hulliger.[10] The structure is composed of $[Re_6Te_8]^{2+}$ clusters linked by butterfly-like units formally written as $\{[\,]Te_6\}Te$, where the last-noted Te is the central one of the unit (**8**). The Te_5^{n-} unit is easily recognized here, however,

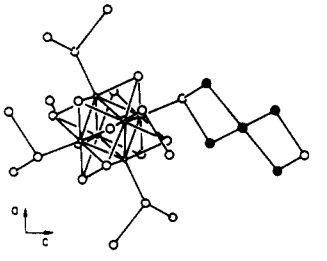

8

(1) Böttcher, P.; Kretschmann, U. *J. Less-Common Met.* **1983**, *95*, 81–91.
(2) Böttcher, P.; Kretschmann, U. *Z. Anorg. Allg. Chem.* **1982**, *491*, 39–46.
(3) Eisenmann, B.; Schwerer, H.; Schäefer, H. *Mater. Res. Bull.* **1983**, *18*, 383–387.
(4) Pauling, L. "The Nature of the Chemical Bond", 3rd ed.; Cornell University Press: Ithaca, NY, 1967; p 246.
(5) Julien-Pouzol, M.; Jaulmes, S.; Alapini, F. *Acta Crystallogr., Sect. B: Struct. Crystallogr. Cryst. Chem.* **1977**, *B33*, 2270–2272.
(6) See, for instance: Cotton, F. A.; Wilkinson, G. "Advanced Inorganic Chemistry"; Wiley-Interscience: New York, 1980; p 347.
(7) Range, K.-J.; Zabel, M.; Ran, F.; von Krziwanek, F.; Marx, R.; Panzer, B. *Angew. Chem., Int. Ed. Engl.* **1982**, *21*, 706–707.
(8) Wang, R.; Steinfink, H.; Bradley, W. F. *Inorg. Chem.* **1966**, *5*, 142–145.
(9) Norling, B. K.; Steinfink, H. *Inorg. Chem.* **1966**, *5*, 1488–1491.
(10) Klaiken, F.; Petter, W.; Hulliger, F. *J. Solid State Chem.* **1983**, *46*, 112–120.

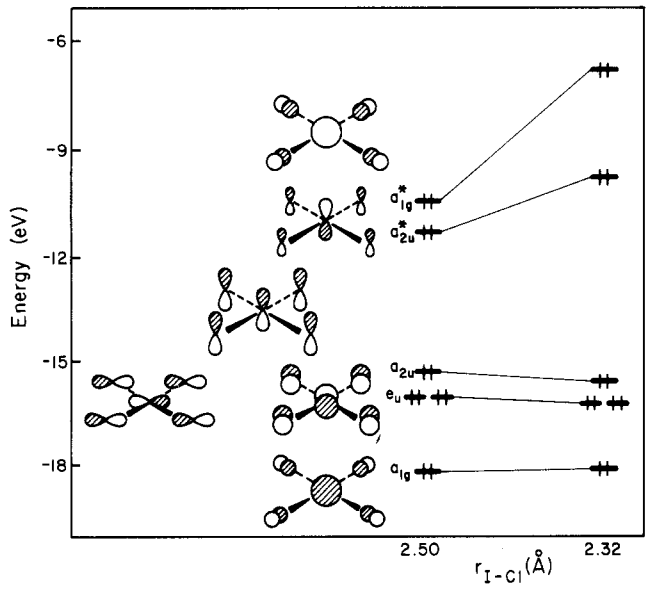

Figure 1. Energy level diagram for ICl_4^- at two different geometries.

and exhibits geometric features characteristic of other units we have already noted.

What are these features? They are summarized in Table I. The variation in geometry among these units is not large, considering the differences in crystalline environment in which they are found. The average Te–Te bond length is 3.039 Å, and except for the one large angle in K_2SnTe_5 they are all essentially square planar in geometry. This characteristic bond length is significantly longer by 0.25–0.30 Å than twice the covalent radius[4] of 1.37 Å, since normal covalent Te–Te bonds fall in the range 2.69–2.80 Å.[11]

The essential questions we wish to address here, then, are as follows: how can the formation of the chain compounds be visualized, and why are the Te(central)–Te(peripheral) bond lengths longer than normal Te–Te bond lengths by ~0.25 Å? We note that the same questions have been recently analyzed in a paper by Bullett.[12]

We turn to the second question first, by recalling an observation we made earlier regarding the $\{SnTe_5^{2-}\}_\infty$ anionic chain. Considering the building blocks of this polymeric chain as Te_5^{6-} and Sn(IV) may at first glance lack chemical aesthetic appeal. However, by analogy with some other well-known species such an approach can lead to an understanding of the bonding in this system.

The square-planar unit is reminiscent of mixed-halogen anions BrF_4^- and ICl_4^- and of XeF_4, an observation already made by others.[2,10] Let us initially examine the first two members of this group. Both are well-documented square-planar structures,[13-15] in which the Br–F bond length is 1.89 (2) Å while I–Cl ranges from 2.42 (1) to 2.60 (1) Å and averages 2.51 (2) Å.[16] These distances are again significantly longer than the respective single-bond distances of Br–F (1.756 Å) and I–Cl (2.321 Å) in the diatomic molecules.[17] This is the same lengthening observed in the Te_5^{n-} units, and its origin is an important point of our story.

The bonding in these molecules is clearly best described in terms of the classical three-center–four-electron bonding model.[18,19] We

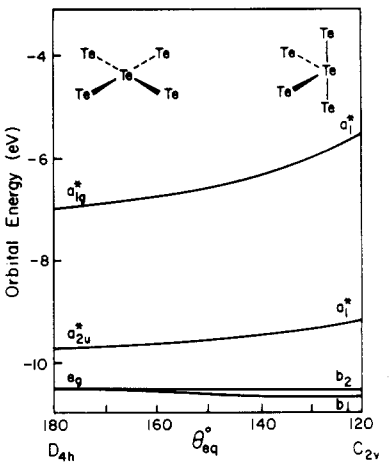

Figure 2. Walsh diagram for the D_{4h}–C_{2v} transformation of the Te_5 unit.

will now discuss in detail the electronic structure of square-planar ICl_4 and Te_5^{n-}.

The energy level diagram for ICl_4^- in D_{4h} symmetry is given in Figure 1. The two highest occupied MO's in this 36-electron system are both antibonding (a_{1g} and a_{2u}) and are clearly destabilizing at a normal I–Cl bond length of 2.32 Å. Their influence, especially that of the a_{1g}, is significantly decreased by extending the bond length to 2.505 Å. Formation of the anion from I^- and four Cl atoms leads to a net decrease in energy of 48.8 kcal/mol per I–Cl bond formed, a value that compares favorably with the literature value of 49.7 kcal/mol.[20] It would appear that lengthening of the I–Cl bonds is required to reduce the antibonding character of the HOMO. An analogy could, in principle, be made with SF_4, which has the C_{2v} trigonal-bipyramid structure with one lone pair of electrons in an equatorial orbital; it is a 34-electron system. The Walsh diagram for the $D_{4h} \rightarrow C_{2v}$ transformation for a Te_5 unit with Te–Te bond lengths of 2.91 Å is given in Figure 2. For a 32-electron count for D_{4h} Te_5^{2-} the e_g level is the HOMO, while for the 36-electron count the a_{1g} level is the HOMO. The filled a_{2u} and a_{1g} orbitals of Figure 1 are not shown in Figure 2. They are just below the e_g level. In the 32-electron case the C_{2v} geometry is more stable by about 0.45 eV. Filling the a_{2u} level for a 34-electron count raises the total energy of the C_{2v} structure by 0.54 eV, barely favoring the D_{4h} geometry. For the 34-electron systems, e.g. SF_4, there is a delicate balance in the calculations between planar and C_{2v} structures.[19] However, the 36-electron count raises the energy of the C_{2v} above the D_{4h} by an additional 1.43 eV, so the latter geometry is clearly preferred.

Let us now carry the analogy directly over to the Te_5^{n-} unit. First, we must take care of the electron count, which again will be 36 if $n = 6$. The formal oxidation state on the central Te is II, considering each of the peripheral Te's as 2–.

When the Te–Te distance is increased from 2.84 to 3.04 Å, the a_{1g} level drops by 2.95 eV and the a_{2u} level drops by 0.4 eV while other levels remain essentially constant. Thus the antibonding character is significantly decreased with almost no loss in bonding character. So why does the Te_5^{6-} unit not exist as an independent entity like ICl_4^- and its analogues? The reason is the difference in electronegativity in the two atom types for ICl_4^- and the lack

(11) See, for instance: Burns, R. C.; Gillespie, W.-C.; Slim, D. R. *Inorg. Chem.* **1979**, *18*, 3086–3094.
(12) Bullett, D. W. *Solid State Commun.* **1984**, *51*, 51–53.
(13) A qualitative treatment of this group has been given: Gimarc, B. M. "Molecular Structure and Bonding"; Academic Press: New York, 1979; Chapter 4. Albright, T. A.; Burdett, J. K.; Whangbo, M.-H. "Orbital Interactions in Chemistry"; Wiley-Interscience: New York, 1985.
(14) Edwards, A.; Jones, G. R. *J. Chem. Soc. A* **1969**, 1936–1938.
(15) Elema, R. J.; De Boer, J. L.; Vos, A. *Acta Crystallogr.* **1963**, *16*, 243–247.
(16) Bateman, R. I.; Bateman, L. R. *J. Am. Chem. Soc.* **1972**, *94*, 1130–1134.
(17) *Spec. Publ.–Chem. Soc.* **1958**, *No. 11*, **1965**, *No. 18*.
(18) (a) Hach, R. J.; Rundle, R. E. *J. Am. Chem. Soc.* **1951**, *73*, 4321–4324. Rundle, R. E. *Ibid.* **1963**, *85*, 112–113. Rundle, R. E. *Surv. Prog. Chem.* **1963**, *1*, 81. (b) Pimentel, G. C. *J. Chem. Phys.* **1951**, *19*, 446–448. (c) Havinga, E. E.; Wiebenga, E. H. *Recl. Trav. Chim. Pays-Bas* **1959**, *78*, 724–738. (d) Gillespie, R. J. *Inorg. Chem.* **1966**, *5*, 1634–1636; *J. Chem. Phys.* **1962**, *37*, 2498; *Can. J. Chem.* **1961**, *39*, 318–323. (e) Musher, J. I. *Angew. Chem., Int. Ed. Engl.* **1969**, *8*, 54–68. (f) Wynne, K. J. "Sulfur Research Trends", 3rd Mardi Gras Symposium, Loyola University, 1971, p 150. An extensive list of references to calculations of the related phosphoranes may be found in the paper by: Hoffmann, R.; Howell, J. M.; Muetterties, E. L. *J. Am. Chem. Soc.* **1972**, *94*, 3047–3058.
(19) See also: Chen, M. M. L.; Hoffmann, R. *J. Am. Chem. Soc.* **1976**, *98*, 1647–1653, and references therein.
(20) Huheey, J. E. "Inorganic Chemistry", 3rd ed.; Harper and Row: New York, 1983; p A-39.

thereof in Te_5^{6-}. The antibonding orbitals a_{1g} and a_{2u} are highly concentrated on the central I atom in the former case (see **9**)

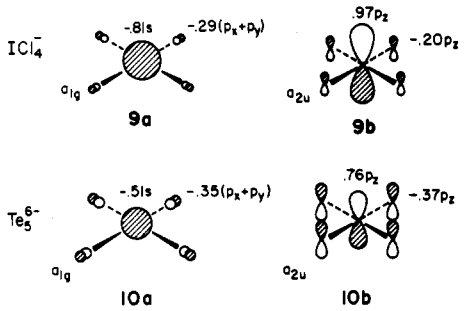

whereas, as expected, there is much less polarization in the Te_5^{6-} case. Thus, in spite of the bond lengthening there is still sufficient antibonding character between central and peripheral Te's to destabilize an individual unit.

There is another factor operating to make XY_4 hypervalent molecules kinetically unstable. Orbitals such as **9** or **10** have substantial electron density on the external Y ligands and are X–Y antibonding. The less electronegative Y is relative to X, the more will such orbitals be localized on the external atoms; these in turn will be activated with respect to electrophiles. The general prescription for kinetic stability for XY_4 molecules of this type is to make the external Y groups as electronegative as possible. In lieu of a large difference in electronegativity electron "pileup" on terminal atoms can be alleviated by forming interfragment bonds.

For Te_5^{6-} stabilization can be achieved by the formation of bonds between units, as in the chain compounds **2** and **3**, or between Te_5^{6-} units and a suitable "mediator" such as Sn. Let us demonstrate how this happens, by first building model molecules from these Te_5^{6-} units, and then extending them to the infinite chains observed.

Let us make the bonding in Te_5^{6-} explicit by structure **11**, which shows the electron pairs as bars. The central Te has four electrons

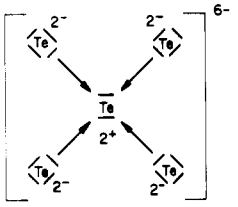

11

in this extreme resonance structure and uses two formally empty p orbitals to engage in electron-rich three-center bonding with the external tellurium atoms. Please do not consider the crude assignment of electrons in **11** as anything but an extreme formalism.

Where are the frontier orbitals **9** and **10**, a_{1g} and a_{21}, in this picture? They are to be identified with the two lone pairs at the central atom in **11**, as approximate as these identifications perforce must be.

The rough formalism illustrated in structure **11** does indicate how a Te_5^{6-} fragment can bond to other entities. If it retains all of its electrons, it can only act effectively as a Lewis base, through either the terminal or central atom lone pairs. This is what it does in **4**, the formal Sn(IV) complex of Te_5^{6-}.

If we allow oxidation of the Te_5^{6-} unit, further bonds may be formed. For instance, one view of the Te_5^{2-} system obtained by removal of four electrons from Te_5^{6-} is shown in **12**. We have

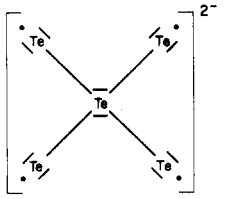

12

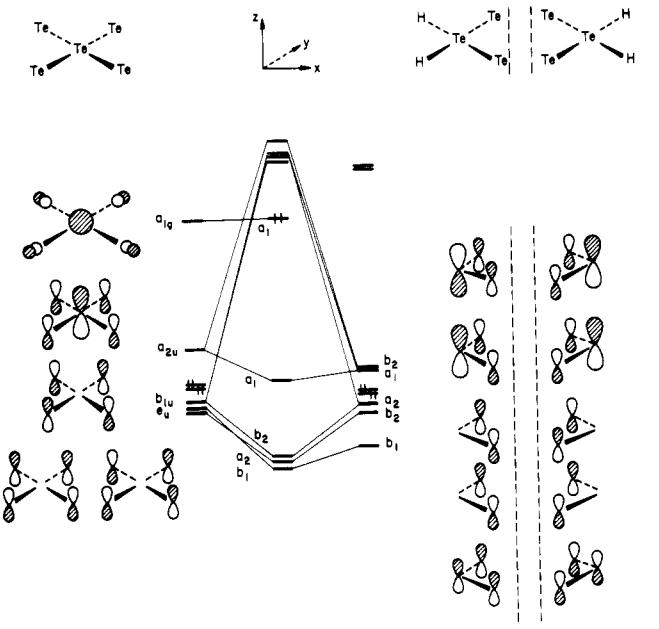

Figure 3. Interaction diagram for **13** and **14**. Only those orbitals on the fragments that interact have been drawn and labeled. The HOMO's for the fragments are also indicated.

chosen to oxidize the terminal tellurium atoms. **12** is a tetraradical, set up to polymerize with itself to form Te–Te bonds and extended structures of type **2** and **3**.

We now return to another approach to the electronic structure of the polymeric $(Te_5^{2-})_n$ chains by examining the bonding in two model compounds, **13** and **14**. We have termed them cisoid and

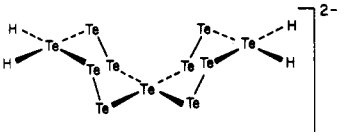

13

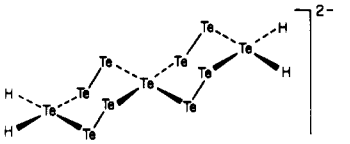

14

transoid, in view of their topological similarity to *cis*- and *trans*-polyacetylene. In the Rb_2Te_5 structure Te–Te bonds within a square-planar unit are 3.04 Å, while those between units are 2.76 Å. An intermediate value of 2.91 Å was chosen for all. All bond angles were chosen as 90° around a central Te atom, while 102.5° was used for the angle around the peripheral atoms.

The entire unit is assigned a charge of 2−. One way to reach this 72-electron count is to begin with a 96-electron trimer $(Te_5^{2-})_3$, which is terminated by four H^- groups instead of Te^{2-}. The 24 lost electrons are essentially the lone pairs on the replaced Te atoms. In an analysis of the bonding in **13** or **14** let us first consider a fragmentation scheme wherein the central Te_5 unit is one fragment and the two peripheral units comprise the second fragment. Again, all Te–Te bond lengths were given an intermediate value of 2.91 Å. Te–H was taken as 1.72 Å.

The interaction diagram is shown in Figure 3. The interaction of the two terminal Te_3H_2 groups with the central Te_5 results in the formation of four Te–Te σ bonds, from the interaction of essentially p_z orbitals. The antibonding combinations are pushed above the a_1 orbital derived from the a_{1g} level of the Te_5 unit, which now becomes the HOMO for the system. This and the second highest filled orbital, also a_1, are both antibonding within the Te_5 unit. The interfragment bonding combinations are not stabilized to the same extent as the destabilization of the intrafragment

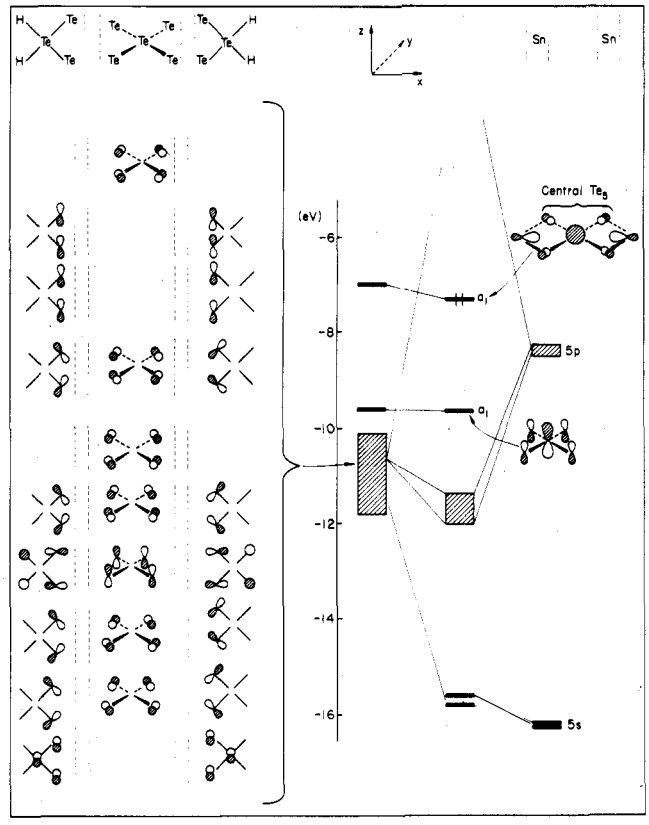

Figure 4. Interaction diagram for **16**.

antibonding combinations. The HOMO's for the fragments are at approximately −10.6 eV while the HOMO for the full molecule is at −6.9 eV. As a result of this large difference, the net effect of forming the molecule is a destabilization of the structure with respect to the two fragments by 1.66 eV. The overall situation may be described as the formation of four σ bonds between units at the expense of filling antibonding orbitals within a unit.

The net positive energy for this process still leaves us with no rationalization for the formation of the compound. Recall that we chose an intermediate value of 2.91 Å for all the Te(peripheral)–Te(peripheral) bond lengths. If we now increase the Te(peripheral)–Te(central) bond length to that observed in the crystal (3.034 Å) and likewise reduce the Te–Te bond length between square-planar units to 2.84 Å, we obtain a net stabilization of 2.2 eV, or about 12.6 kcal per Te–Te bond. The stabilization is due principally to a lowering of the HOMO (by 1.3 eV). This rather dramatic change with geometry demonstrates the strong competition between the antibonding character of the Te_5^{6-} unit discussed earlier and the stabilization obtained by forming chains of these units.

The difference in the nature of the Te–Te bonds in this model for a polymer was already foreshadowed in the electronic structure of the initial model, with all Te–Te distances equal. The overlap populations computed there were 0.155 within the square-planar unit and 0.449 between units. This is a large difference, reflecting the weaker electron-rich three-center bonding. It is no wonder that the bonds to the square-planar coordinated Te elongate.

Further evidence for this driving force for Te(central)–Te(peripheral) bond elongation may be derived from a calculation in which the fragmentation is chosen to examine the effect of bonding within these square-planar units, rather than between them, in the stabilization of the chain structure. One fragment would be the four ditelluride (Te–Te) units that make up the links between square-planar units, while the remainder of the molecule (two TeH_2 units plus Te) comprises the second fragment. For the geometry with all Te–Te bonds of 2.91 Å, the bringing together of these fragments (formation of bonds within square-planar Te_5 units) is unstable with respect to the fragments by 3.52 eV. Recall that relaxation of the geometry to that found in the crystal for the square-planar fragmentation did result in a net stabilization of 2.2 eV. The same process for this fragmentation still does not suggest a net bonding situation—the energy of the whole is 1.24 eV higher than the sum of the fragments.

In summary, the square-planar Te_5^{6-} system can find a way of overcoming a delicately balanced but essentially antibonding situation by losing four electrons and by forming bonds between neighboring units. Now that we have seen the basis for the formation of bonds between square-planar units, we wish to ask if the geometry also plays an important role in this process, for we have already seen that even a homoatomic chain can adopt at least two different geometries, **13** and **14**. For the transoid model compound, **14**, the interaction diagram is virtually identical with that for the cisoid, **13**, already discussed. This is not unreasonable: the structure is stabilized by the formation of σ bonds between essentially D_{4h} units, and the propagation of these bonds "above" or "below" the plane would seem to be equally possible on an energetic basis. The only real difference in interatomic interactions between the two molecules is a possible through-space Te···Te interaction indicated in **15**. But the distance is nearly 6 Å, so this may be ignored.

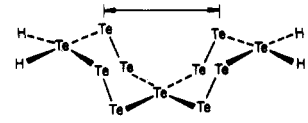

15

We are now in a position to look at the $SnTe_5^{2-}$ chain, **4**, and again we choose a model compound, **16**, to get some idea of the bonding in this system. We suggested earlier two possible ways

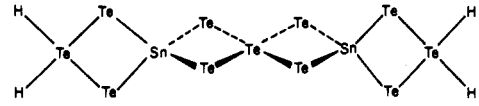

16

of thinking about the electron count: either as a combination of Sn^0 and Te_5^{2-} units or as Sn(IV) and Te_5^{6-}. In light of what has been said above, clearly there is a preference for the second choice.

Calculations were carried out for two geometries, **17a** and **17b**. The restrictions of 90° bond angles around the central Te and Te–Sn bond lengths of 2.78 Å determine the Te–Te–Sn and Te–Sn–Te bond angles. In the experimental structure the Te–

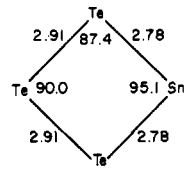

17a

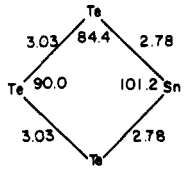

17b

Te–Te angles within a Te_3Sn ring are 88.5 and 95.0° while exocyclic ones are 88.5°. The angles about the Sn are 102.1, 103.9, and 112.8° (4×) so strict square-planar geometry is not obtained in the former case and ideal tetrahedral geometry is not obtained in the latter case.

The interaction diagram for a fragmentation into planar Te_5 (and two planar Te_3H_2 units) in one fragment and two Sn in the second fragment for geometry **17a** is given in Figure 4. A pattern similar to that which we encountered earlier for **13** is observed here as well. Eight bonding orbitals are only slightly lowered with respect to their energy in the Te_5 and Te_3H_2 fragments, but the antibonding orbitals are pushed way above the by now familiar antibonding a_1 orbital within the central Te_5 unit, which becomes the HOMO. The lowest antibonding combination can be found at +0.59 eV. Note that the HOMO is lowered by ~0.25 eV upon formation of the molecule due to a small contribution from the p_x orbital of the Sn, which leads to some Te(peripheral)–Te(peripheral) bonding character. When the geometry is altered to **17b**, increasing the bonded Te–Te distance and decreasing the inter-

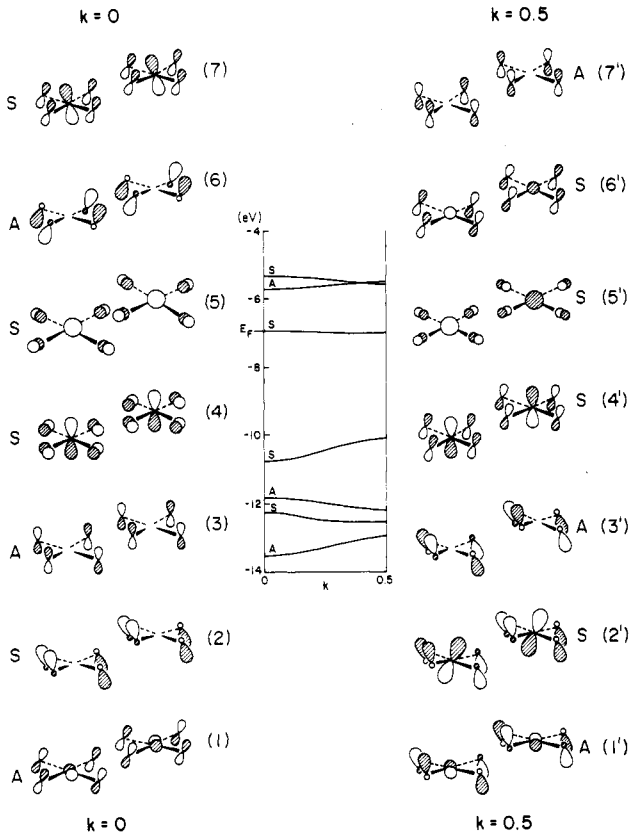

Figure 5. Band structure for the transoid Te_5^{2-} chain.

action between peripheral Te's through the Sn in the HOMO, the HOMO is lowered by 1.25 eV, indicating again the importance of the antibonding character within this unit. However, the block of bonding orbitals at ~11.5 eV does not contain any contribution to bonding *within* Te_5 units.

The formation of the molecule from these two fragments with geometry **17a** yields a net binding energy of 15.3 eV or 44 kcal per Sn–Te bond formed. Relaxation to the geometry of **17b** yields 18.5 eV or 53 kcal per Sn–Te bond. The molecule may also be fragmented as in **18** to examine the effect of the formation of

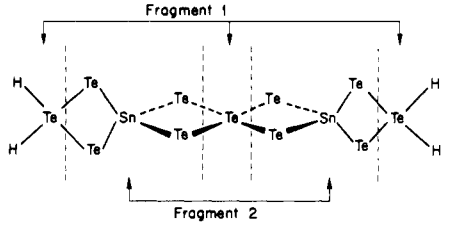

18

Te(central)–Te(peripheral) bonds. With a charge of 2– on the central Te the net binding energy (for the formation of eight Te–Te bonds) is 0.56 eV, for the geometry in **17a**. Clearly the first fragmentation scheme with the geometry in **17b** is preferable in accounting for the bonding in this model compound.

We are now ready to examine the extended systems containing Te_5 units. The band structure for the transoid Te_5^{2-} chain **3** is shown in Figure 5. The Fermi level is at −6.95 eV (k = 0) corresponding to the energy of the HOMO in the trimer **14**. There is very little dispersion in this band due to the near-orthogonality of the now familiar orbitals on the peripheral Te's at both edges of the Brillouin zone.

Two bonds are formed per unit cell (or more correctly between unit cells as defined here), so by analogy with the molecular unit we expect two essentially antibonding levels above the Fermi level; these appear at −5.71 and −5.33 eV, respectively. The material is thus expected to be a semiconductor with band gap 1.24 eV at k = 0.

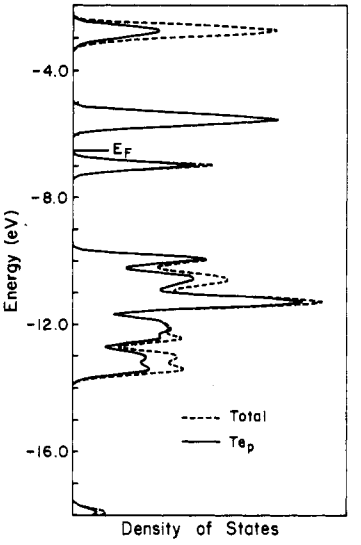

Figure 6. Density of states for the transoid Te_5^{2-} chain.

Figure 5 shows only those bands that are important in Te–Te bonding. Omitted from the figure, for reasons of clarity, are several bands between −9.8 and −13.5 eV, which are composed mainly of nonbonding orbitals. The important interactions at the edges of the Brillouin zone are summarized in Figure 5. The antibonding orbitals appear in symmetric and antisymmetric combination with respect to the mirror plane of the chain as in **19**.

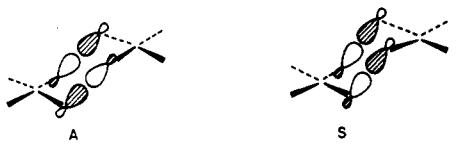

19

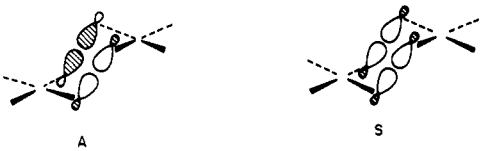

20

Then, we expect two bonding bands, again corresponding to the A and S combinations in **20**. In fact, four bands may be associated with the bonding due to rather extensive mixing between bands at the edges of the Brillouin zone. The highest S antibonding band at k = 0 (7) correlates with the highest bonding band at k = 0.5 (4′). The latter is, in turn, antibonding with respect to its origin at k = 0 due to the presence of antibonding interactions within the Te_5 unit. The symmetric antibonding band at k = 0 (6) also correlates with the lower S bonding band at k = 0.5 (2).

As one starts from k = 0.5 for the S antibonding band (6′) there is a correlation with the lower S bonding band at −12.1 eV (2). These correlations from antibonding to bonding bands lead to avoided crossings which account for the change in topology of the band orbitals in moving across, e.g., a bonding band.

A similar correlation may be made for the antisymmetric bands. The antibonding one at k = 0 (6) correlates with the higher bonding one at k = 0.5 (3′) while the lower A band at k = 0 (1) correlates with A antibonding at k = 0.5 (7′).

Associated with the band structure of the transoid chain is the density of states (DOS) in the polymer. This is plotted in Figure 6, along with a partitioning that shows the contribution of the four peripheral telluriums. The remainder in the DOS curve is the contribution of the single central Te. The total charge on a peripheral Te atom is −0.587, and that on the central Te is +0.348.

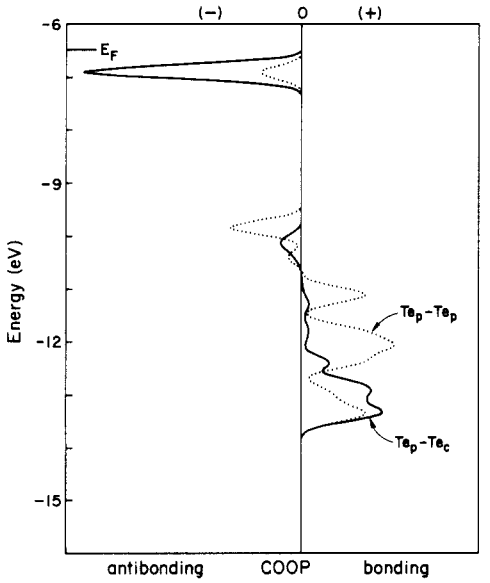

Figure 7. Crystal orbital overlap population (COOP) curves for the two different Te–Te bonds in the Te_5^{2-} chain.

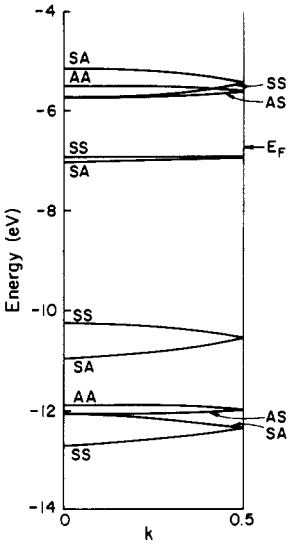

Figure 8. Band structure of the cisoid Te_5^{2-} chain. Only bands contributing to Te_5···Te_5 interaction are included. The two-letter symmetry classifications refer to the mirror plane parallel to the chain propagation direction and the 2_1 screw axis.

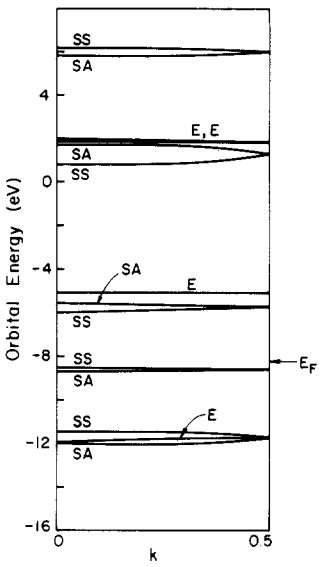

Figure 9. Band structure for the $SnTe_5^{2-}$ chain. The two-letter symmetry classifications refer to the mirror plane parallel to the chain propagation direction and the 4_2 screw axis. E refers to a degenerate pair of bands.

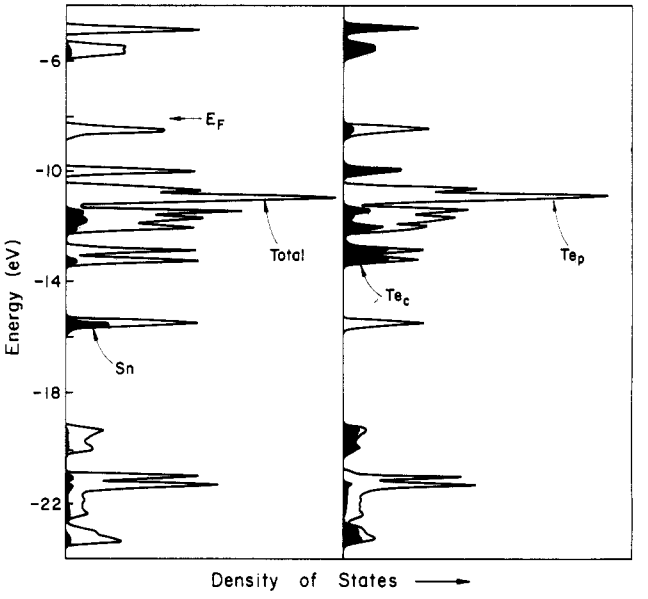

Figure 10. Total density of states and contributions from the three different atom types in the $SnTe_5^{2-}$ chain.

This is the same trend as in the Te_5 model.

The total overlap populations in the polymer are 0.155 for Te_c–Te_p and 0.429 for Te_p–Te_p, where the subscripts c and p stand for central and peripheral, respectively. A more detailed decomposition of the bonding is obtained through COOP curves. These are overlap-population-weighted densities of states, i.e. DOS curves in which the relative number of states in a given interval is weighted by the contribution that those states make to bonding or antibonding for a specified bond. We have found these COOP curves most useful for analyzing bonding trends.[21] A COOP curve for the Te_5^{2-} polymer is shown in Figure 7. Note that the highest occupied band in the polymer is both Te_p–Te_p and Te_c–Te_p antibonding, especially so in the latter bond. The antibonding nature of the model and the polymer has been discussed earlier. It is interesting to speculate here that a material with stronger Te–Te bonding could be made if one could oxidize the Te_5^{2-} chain. For instance, the total overlap for the Te_c–Te_p and Te_p–T_p bond rises to 0.373 and 0.471, respectively, upon reducing the electron count from 32 to 30 electrons per Te_5 unit.

The similarity between the model cisoid and transoid molecules **13** and **14** is expected to be maintained in the extended structures as well. The major difference is the presence of the additional screw-axis element in the cisoid chain, causing the repeat distance to double. The symmetry of the chain is thus nonsymmorphic, resulting in a "folding back" of the bands, as seen in Figure 8. Again, only those bands that contribute to bonding between Te_5 units have been included. The topology of the orbitals is the same for both structures. Indeed, if we could "unfold" the bands for the cisoid polymer, the two band structures would be essentially superimposable.

The band structure for the $SnTe_5^{2-}$ chain (Figure 9) shows even less dispersion than the pure Te_5 chains. The band gap in this case is 2.66 eV, again indicating a semiconductor. Following the model molecule **16**, the conduction band (~−5.5 eV) is composed of nonbonding orbitals on the tellurium atoms. The band structure has been simplified here by eliminating all nonbonding orbitals except those in the conduction band. A discussion similar to that given for the pure Te_5 chains relating to the avoided crossings could

(21) These curves were invented by S. Wijeyesekera in our group. For some applications see: (a) Hughbanks, T.; Hoffmann, R. *J. Am. Chem. Soc.* **1983**, *105*, 3528–3537. (b) Kertesz, M.; Hoffmann, R. *Ibid.* **1984**, *106*, 3453–3460. (c) Saillard, J.-Y.; Hoffmann, R. *Ibid.* **1984**, *106*, 2006–2026.

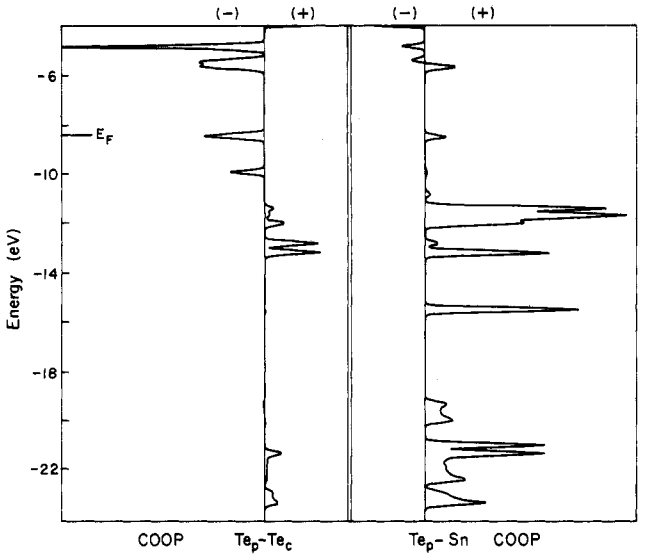

Figure 11. COOP curves for the two bond types in the $SnTe_5^{2-}$ chain.

be given here; however, the bonding in the chain can be understood on the basis of the model compound **16** discussed above.

The total density of states of $SnTe_5^{2-}$ is shown in Figure 10. Note the relatively small contribution of Sn to the DOS; this is consistent with the large positive charge calculated on Sn of 1.13 and the formal assignment of a +IV oxidation state. The highest occupied band is almost entirely on Te. It represents mainly the nonbonding electrons that have been depicted earlier in Figure 7. There are some differences between our band structure and that computed by Bullett,[12] but there are more similarities: the absence of Sn character in the highest band and the concentration of Sn in a band ~7 eV below the Fermi level.

The COOP curves in Figure 11 reflect the pattern already discerned in the model compound: below the Fermi level the interaction between peripheral Te and Sn is all bonding; the Te(central)–Te(peripheral) overlap populations are bonding to ~−11 eV, but from there to the Fermi level there are two strong antibonding orbitals in the molecular model.

The fact that the topmost filled bands are strongly antibonding within a Te_5 unit suggests that oxidation of the chain would lead to shorter Te–Te bands within that unit. With the Fermi level at ~−7 eV oxidation is not excessively difficult and all three chains with a formal building unit of Te_5^{x-} ($-2 < x < 0$) might be attainable with proper choice of synthetic conditions. All three known compounds were obtained by heating stoichiometric quantities of the elements involved;[1-3] compounds such as Rb_2Te_5 and K_2SnTe_5 with the lower electron count on the Te_5 unit might result from starting materials in the proper stoichiometric ratios.

The symmetry properties of the chains aid in understanding the location of the cations with respect to the central Te of a Te_5 unit. In the cisoid and transoid all-Te chains **2** and **3** the cations (Cs and Rb, respectively) are located on axes perpendicular to the Te_5 unit. In **2** the Cs–Te distances are 3.92 and 3.96 Å while in **3** the Rb–Te distance is 3.88 Å.

In the K_2SnTe_5 structure the K^+ cations lie on an axis that runs through the central Te but in preservation of the symmetry of the tetragonal space group *I4cm* is at a 45° angle to the Te_5 plane. The Te–K distance is 4.24 Å. In fact, the cation is closer to the two peripheral Te's with distances of 3.52, 3.59, 3.71, and 3.80 Å.

The difference in the geometry of cation arrangement around the chains may be understood on the basis of the symmetry properties of the chains in the three structures. In the cisoid chain the plane of the Te_5 unit is not a mirror plane of symmetry of the entire chain. Consequently the HOMO and the orbital below it mix to form a pair of hybrid sp type orbitals (**21a** and **21b**) at the central Te. Thus there is a concentration of electron density along this axis and, not unexpectedly, the two cations for each Te_5 unit are located on this axis. In this chain there must be an

21a **21b**

asymmetric top–bottom distribution of axial density at Te_c—and this might account for the 0.04-Å difference in Te_c–Cs distances. The longer Te_c–Cs distance is to Cs(2), which caps the "boat" formed by a Te_5 unit and the four Te_p's bonded to it. The distances between these last four Te_p's and Cs(2) are all equal and are the shortest Te–Cs distance (3.85 Å), resulting in C_{4v} local symmetry and suggesting a chelating effect of these Te_p's. Indeed, one of the lone-pair lobes on these atoms does point toward the inside of the "boat" and is certainly sufficiently diffuse to interact with the Cs cation.

The presence of an inversion center at Te_c in the transoid chain prevents s, p_z mixing; however, it does require equal Te_c–Rb distances above and below the Te_5 plane. Similarly, there is no physical basis for mixing as in **21** since the Te_5 units lie on a mirror plane. There is less of a concentration of electron density on Te_c, and the alternate location of the cation is preferred.

Another interesting feature of the structures is the short Te···Te interchain distance of 3.47 Å found in the transoid structure. Short distances such as this are found in many tellurium and selenium structures where steric factors do not prevent the close approach of these atoms. For instance, in α-tellurium, the helical chains have Te–Te bond lengths of 2.83 Å, but each tellurium has four neighbors at distances of 3.494 Å.[22]

The geometric nature of the interaction between transoid chains is shown in **22** and **23**. **22** indicates in a side view the short

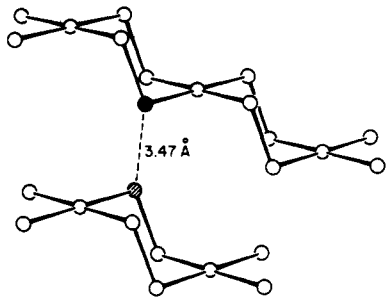

22

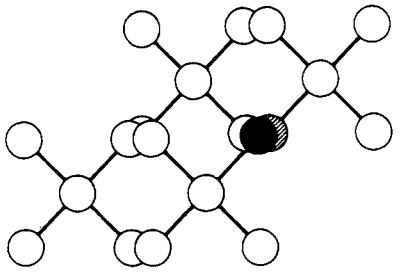

23

contact. In **23** the same structure is shown in projection onto the plane of a Te_5 unit. One atom has been darkened and another shaded to aid in identifying the interaction. **23** in particular strongly suggests an interaction between p_z-type orbitals.

Calculations were carried out on a "dimer" composed of two molecules of **14**. For the geometry as shown in **22** the dimer is not bound with respect to the two monomers by 0.47 eV. Shifting the molecules closer to 3.27 Å leads to a worse situation where the difference is ~1 eV. A lateral shift of the chains to bring the two interacting atoms into an eclipsed orientation does not

(22) Cherin, P.; Unger, P. *Inorg. Chem.* **1967**, *6*, 1589–1591.

Table II. Extended Hückel Parameters

orbital		H_{ii}, eV	exponent
Te	5s	-20.78	2.51
	5p	-11.04	2.16
Sn	5s	-16.16	2.13
	5p	-8.32	1.82
H	1s	-13.60	1.30

lead to any significant improvement. Interestingly, the reduced overlap populations for atoms that might be involved in this interaction show that indeed there is a small bonding interaction (+0.0039) but there is an antibonding one of similar magnitude (-0.0037) between the darkened Te and the central Te in the Te_5 unit containing the shaded Te. These two interactions are of similar magnitude in all the other geometries. As we move the two trimers toward each other, past the equilibrium separation in the polymer, the Te_p-Te_p' interaction grows more bonding but the above-mentioned Te_p-Te_c' interaction becomes more antibonding. The total energy for the approach of the two trimers is quite repulsive. It appears that our method does not portray properly the origins of what we feel on structural grounds must be a bonding interaction.

In summary, we have examined the electronic structure and bonding in a number of polymers containing the square-planar Te_5 repeating unit. These are seen to be characterized by weaker electron-rich three-center bonds within the unit, which accounts for the elongation of the intraunit Te-Te bond length by ~0.25 Å over a normal bond, and the unit is shown to be an unstable species, compared with, e.g., ICl_4^-. However, the formation of infinite one-dimensional chains due to covalent or dative bonding between units (Te_5^{2-}) or with another modulating atom ($SnTe_5^{2-}$) is energetically sufficient to stabilize the overall structure. In spite of the significant topological difference between the Cs_2Te_5 (cisoid) and Rb_2Te_5 (transoid) chains their electronic structures are virtually identical. These have been interpreted for all three compounds by employing model molecules, which provided a basis for understanding the band structure of the infinite chains. The HOMO in the model compounds is an antibonding orbital within the square-planar unit, leading to the suggestion that modification of the synthesis of these compounds could lead to an oxidized form of the chain with modified properties and greater inherent stability of the Te_5^{n-} units. The electronic basis for the short interchain Te···Te distance of 3.47 Å, reminiscent of a similar contact in elemental tellurium, was investigated but apparently is beyond the capability of the extended Hückel method.

Acknowledgment. J.B. wishes to thank S. Alvarez and J. Silvestre for many helpful discussions. We are grateful to Eleanor R. Stagg for typing the manuscript and to Jane Jorgensen for the figures. Our work was supported by NSF Grant CHE8406119. We have benefited greatly from the comments of a careful and conscientious reviewer. Many of his or her suggestions have been included in the final version of the manuscript.

Appendix

Extended Hückel parameters for all atoms used are presented in Table II. The H_{ii} values are from ref 23, and the exponents are from ref 24.

Registry No. Rb_2Te_5, 88188-94-7; Cs_2Te_5, 83332-22-3; K_2SnTe_5, 86205-22-3; Te, 13494-80-9.

(23) Hinze, J.; Jaffé, H. H. *J. Am. Chem. Soc.* **1962**, *84*, 540-548.
(24) Clementi, E.; Roetti, C. *At. Data. Nucl. Data Tables* **1974**, *14*, 177-478.

Contribution from the Department of Chemistry and Materials Sciences Center, Cornell University, Ithaca, New York 14853

Tetrahedral and Square-Planar One-Dimensional Chains: The Interplay of Crystal Field and Bandwidth in MS_2 Compounds

JÉRÔME SILVESTRE and ROALD HOFFMANN*

Received March 29, 1985

One-dimensional ML_2 chains with edge-sharing tetrahedral or square-planar coordination at the transition metal are the subject of this theoretical analysis. The band structures of these systems are examined in substantial detail. The local ligand field at the metal is a good starting point for an understanding of the band ordering in these extended structures, but inter unit cell interactions, both through the bridges and directly between the metals, are important for setting the energy order and dispersion of the bands and especially for determining unexpected electron counts for semiconducting behavior; one such case is d^6 for the tetrahedral chain. Pairing distortions, chain folding, and uniform contractions and elongations are also studied in some detail for these materials.

The two most frequency encountered geometrical arrangements of four ligands L around a metal atom are tetrahedral (**1**) or square planar (**2**); the complex stoichiometry in both cases in ML_4. If

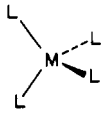

1

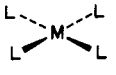

2

the ligand L has the ability to function as a bridge between two metal centers, it is in principle possible to generate from **1** and **2** the polymers **3** and **4**, respectively. The stoichiometry of these

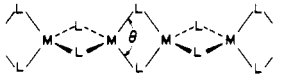

3

4

chains is $ML_{4/2}$ or ML_2. The magnificent world of structural solid-state chemistry shows us that infinite systems such as **3** and **4** are not just the fruit of our imagination: they do occur in reality.[1]

Table I. Some Known ML_2 Structures

compd	chain	type	θ, deg	M-M, Å	d^n	ref
$KFeS_2$	FeS_2^-	**3**	106.0	2.70	d^5	2a
$RbFeS_2$	FeS_2^-	**3**	105.0	2.71	d^5	2b
$CsFeS_2$	FeS_2^-	**3**	105.0[a]	2.71[a]	d^5	2b, 3
$Na_3Fe_2S_4$	$FeS_2^{1.5-}$	**3**	106.0	2.75	$d^{5.5}$	4
$Na_5Co_2S_5$	$CoS_2^{1.5-}$	**3**	96.0	3.11	$d^{6.5}$	5
Na_2PdS_2	PdS_2^{2-}	**4**	82.5	3.54	d^8	6
Na_2PtS_2	PtS_2^{2-}	**4**	82.5	3.55	d^8	6
K_2PtS_2	PtS_2^{2-}	**4**	81.0	3.59	d^8	7
Rb_2PtS_2	PtS_2^{2-}	**4**	79.1	3.64	d^8	7
α-$PdCl_2$	$PdCl_2$	**4**	87.0	3.34	d^8	8

[a] Average value.

(1) Bronger, W. *Angew. Chem.* **1981**, *93*, 12; *Angew. Chem., Int. Ed. Engl.* **1981**, *20*, 52.

0020-1669/85/1324-4108$01.50/0